Letter

Emergent skyrmion-based chiral order in zero-field Heisenberg antiferromagnets on the breathing kagome lattice

Kazushi Aoyama[1] and Hikaru Kawamura[2]

[1]*Department of Earth and Space Science, Graduate School of Science, Osaka University, Osaka 560-0043, Japan*
[2]*Molecular Photoscience Research Center, Kobe University, Kobe 657-8501, Japan*

We show that classical Heisenberg antiferromagnets on the breathing kagome lattice can be a platform to realize a zero-field topological order of the scalar spin chirality which can be viewed as a miniature skyrmion crystal (SkX) of discrete form with a small number of spins in its magnetic unit cell. In the model, a third nearest-neighbor (NN) antiferromagnetic interaction along the bond direction J_3 and the breathing bond alternation characterized by the ratio of the NN interaction for large triangles to that for small ones, J_1'/J_1, are essential. It is found by means of Monte Carlo simulations that a commensurate triple-$\mathbf{Q}$ state appearing for relatively strong J_3 at zero field is the noncoplanar state with the SkX structure in the breathing case of $J_1'/J_1 \neq 1$, while in the uniform case of $J_1'/J_1 = 1$, it is a collinear state favored by thermal fluctuations. The origin of this chiral order and experimental implications of our result are also discussed.

DOI: 10.1103/PhysRevB.105.L100407

In magnetic materials, the scalar spin chirality $\mathbf{S}_1 \cdot (\mathbf{S}_2 \times \mathbf{S}_3)$ defined by three localized spins $\mathbf{S}_i$ often plays an important role. In particular, when a total chirality summed over the whole system is finite, the underlying noncoplanar spin state can be topologically nontrivial in the sense that the spin structure itself and/or the band structure of coupled electrons are characterized by nonzero integer topological numbers [1–4]. Such a chiral order is known to occur at zero field in two dimensions with its origin being multispin interactions [5] or a coupling to conduction electrons [2–4,6]. In this Letter, we theoretically show that a breathing bond alternation of the lattice serves as another mechanism leading to an exotic zero-field chiral order which can be viewed as a miniature version of a skyrmion-crystal (SkX) topological spin texture.

The SkX is a two-dimensional periodic array of magnetic skyrmions, each of which is characterized by an integer topological number corresponding to the total solid angle subtended by all the spins, $n_{\rm sk} = \frac{1}{4\pi} \sum_{i,j,k} \Omega_{ijk}$ [1]. Since the solid angle for three spins Ω_{ijk} is related with the chirality $\chi_{ijk} = \mathbf{S}_i \cdot (\mathbf{S}_j \times \mathbf{S}_k)$ via $\Omega_{ijk} = 2 \tan^{-1}[\frac{\chi_{ijk}}{|\mathbf{S}_i||\mathbf{S}_j||\mathbf{S}_k| + \sum_{\rm cyclic} \mathbf{S}_i \cdot \mathbf{S}_j |\mathbf{S}_k|}]$ [7], the SkX can be understood as a topological chiral order. The SkX is usually realized in an applied magnetic field irrespective of whether the Dzyaloshinskii-Moriya (DM) interaction is present [8–24] or not [25–41]. Recently, it was pointed out that the SkX can be stable even at zero field due to a coupling to conduction electrons on the triangular lattice [30,31]. In view of such a situation, we search for a two-dimensional zero-field chiral order as a candidate for a zero-field SkX.

Since on the three-dimensional pyrochlore lattice having kagome-lattice layers as a building block, a noncoplanar topological spin texture called the hedgehog lattice [42–49] is induced at zero field by the combined effect of a third nearest-neighbor (NN) antiferromagnetic interaction along the bond direction J_3 and a breathing bond alternation of the lattice [50], it is naively expected that in the associated two-dimensional system, i.e., J_3-rich antiferromagnets on the breathing kagome lattice, a noncoplanar spin state may possibly be realized at zero field. Inspired by this idea, we consider the J_1-J_3 classical Heisenberg model on the breathing kagome lattice consisting of an alternating array of corner-sharing small and large triangles.

For the uniform kagome lattice only with the NN antiferromagnetic interaction J_1, it is well established that spins do not order even at $T = 0$ due to a massive ground-state degeneracy resulting from frustration. By introducing additional interactions, three kinds of 12-sublattice noncoplanar states can be stabilized at zero field. Among the three, two are cuboc states induced by further NN interactions, but they are not the SkX, as the total chirality summed over the triangles vanishes [51–53]. The remaining one is a uniform chiral order induced by the coupling to conduction electrons (see Fig. 4 in Ref. [4]). Although this chiral order is topologically nontrivial, it appears only for a special electron filling. The main finding of this work is that a similar but different 12-sublattice uniform chiral order taking a SkX structure is stabilized by the breathing lattice structure at zero field in the presence of relatively strong J_3.

The spin Hamiltonian we consider is given by

$$\mathcal{H} = J_1 \sum_{\langle i,j \rangle_S} \mathbf{S}_i \cdot \mathbf{S}_j + J_1' \sum_{\langle i,j \rangle_L} \mathbf{S}_i \cdot \mathbf{S}_j + J_3 \sum_{\langle\langle i,j \rangle\rangle} \mathbf{S}_i \cdot \mathbf{S}_j, \quad (1)$$

where $\langle \rangle_{S(L)}$ denotes the summation over site pairs on small (large) triangles. The ratio between the NN interactions on the small and large triangles J_1 and J_1', J_1'/J_1, measures the strength of the breathing bond alternation. The third NN
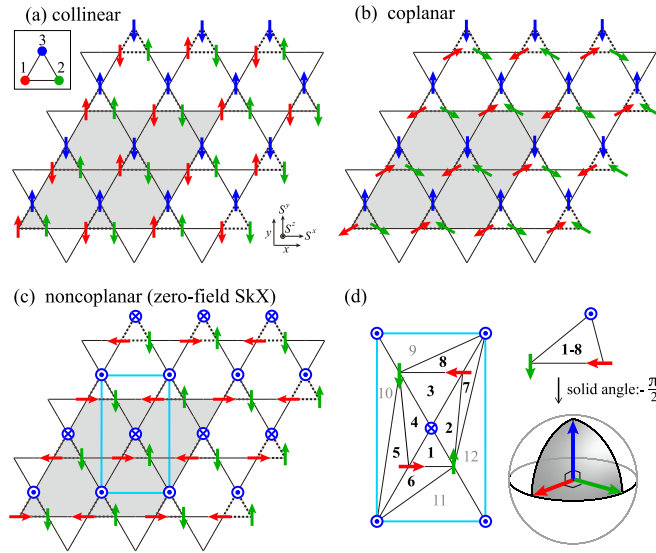
FIG. 1. Schematically drawn spin structures of the three triple-**Q** states. (a) Collinear, (b) coplanar, and (c) noncoplanar SkX states, where red, blue, and green arrows, respectively, represent spins on the corners of 1, 2, and 3 of the small triangle shown in the inset. All three are 12-sublattice states whose magnetic unit cell is indicated by a gray-colored region. In (c), a cyan rectangle indicates a single skyrmion whose enlarged view is shown in (d). In (d), the solid angle spanned by three spins on each of 1–8 triangles is $-\frac{\pi}{2}$, whereas those for 9–12 triangles are zero.

interaction along the bond direction J_3 is fixed to be positive (antiferromagnetic), whereas J_1 and J_1' may be positive or negative. For the occurrence of the zero-field chiral order, the signs of J_1 and J_1' do not matter as long as antiferromagnetic J_3 is sufficiently strong.

We investigate the ordering properties of the Hamiltonian (1) by means of Monte Carlo (MC) simulations. In this work, 2×10^5 MC sweeps are carried out and the first half is discarded for thermalization, where our one MC sweep consists of one heat-bath sweep and successive ten overrelaxation sweeps. Observations are done at every MC sweep, and the statistical average is taken over four independent runs. The total number of spins N is related with a linear system size L via $N = 3L^2$. By measuring various physical quantities, we identify low-temperature phases. For relatively strong J_3, a 12-sublattice triple-**Q** state, characterized by the three commensurate ordering vectors of $\mathbf{Q}_1 = \frac{\pi}{2a}(-1, -\frac{1}{\sqrt{3}})$, $\mathbf{Q}_2 = \frac{\pi}{2a}(1, -\frac{1}{\sqrt{3}})$, and $\mathbf{Q}_3 = \frac{\pi}{2a}(0, \frac{2}{\sqrt{3}})$ with side lengths of each triangle a, appears, and it takes three different spin configurations, collinear, coplanar, and noncoplanar structures, depending on the value of J_1'/J_1. The noncoplanar state corresponds to a zero-field SkX state.

In the present two-dimensional Heisenberg-spin model, a long-range magnetic order is not allowed at any finite temperature, but the spin correlation develops over more than 500 lattice spacings even just below the transition. Below, we will discuss the structures of the spins which are not long-range ordered but correlated over a sufficiently long distance.

Figure 1 illustrates the three triple-**Q** states, where their elementary unit is the small triangle whose three corners will

be called sublattice 1, 2, and 3 [see the inset of Fig. 1(a)]. A common feature of the three triple-**Q** states is that spins residing on each sublattice, which are represented by the same color arrows in Fig. 1, constitute $\uparrow\downarrow\uparrow\downarrow$ chains running along the bond directions, although in reality $\uparrow$ and $\downarrow$ spins are slightly tilted in the noncollinear states (for details, see Supplemental Material [54]). Suppose that the spin polarization vector of the $\uparrow\downarrow\uparrow\downarrow$ chain on sublattice μ is $\hat{P}_\mu$. Then, the difference in the three triple-**Q** states consists in the relative angles among $\hat{P}_1$, $\hat{P}_2$, and $\hat{P}_3$. In the collinear (coplanar) state shown in Fig. 1(a) [Fig. 1(b)], $\hat{P}_1$, $\hat{P}_2$, and $\hat{P}_3$ are in the same direction (plane). In the noncoplanar state shown in Fig. 1(c), $\hat{P}_1$, $\hat{P}_2$, and $\hat{P}_3$ are orthogonal to one another, and six spins form a single skyrmion [see the cyan rectangle in Fig. 1(c)]; a center spin is pointing down, the outer spins are pointing up, and in between, four spins form a vortex. Since it involves only a fixed small number of spins on the discrete lattice sites, it may be called a miniature skyrmion of discrete form, being distinguished from the conventional skyrmion. As one can see from Fig. 1(d), the miniature skyrmion is tiled up with 12 triangles, among which only the inner eight [1–8 in Fig. 1(d)] have a nonzero solid angle of $-\frac{\pi}{2}$ because each triangle has three orthogonal spins. Thus, the total solid angle is $-\frac{\pi}{2} \times 8 = -4\pi$, which is consistent with the definition of the skyrmion with $n_{\text{sk}} = -1$, where the minus sign enters as χ_{ijk} is defined in the anticlockwise direction. Since this skyrmion consists of six spins, the skyrmion number per 12-sublattice magnetic unit cell is $n_{\text{sk}} = \pm 2$. We note that on the *uniform* kagome lattice, this noncoplanar state is not realized [57,58], but is called a octahedral state in Refs. [57,58]. Bearing in mind the above spin structures, we will turn to the result of our MC simulations.

Figure 2(a) shows the temperature dependence of the specific heat C, the spin collinearity $P = \frac{3}{2}\langle \frac{1}{N^2} \sum_{i,j} (\mathbf{S}_i \cdot \mathbf{S}_j)^2 \rangle - \frac{1}{3}\rangle$, the total scalar chirality $|\chi^{\text{T}}| = \langle \frac{1}{2L^2} |\sum_{i,j,k\in\triangle,\triangledown} \chi_{ijk}|\rangle$, and the skyrmion number per magnetic unit cell $|n_{\text{sk}}| = \frac{1}{4\pi}\langle \frac{1}{N/12} |\sum' \Omega_{ijk}|\rangle$ for various values of J_1'/J_1 at $J_3/J_1 = 1.2$ with $J_1 > 0$, where $\langle \mathcal{O} \rangle$ denotes the thermal average of a physical quantity $\mathcal{O}$. In $|n_{\text{sk}}|$, $\sum'$ denotes the summation over all the triangles that tile up the whole system, and Ω_{ijk} is evaluated by using spin configurations averaged over 10 MC sweeps to reduce the thermal noise.

In the uniform case of $J_1'/J_1 = 1$ [see greenish symbols in Fig. 2(a)], the collinearity P develops below a transition temperature indicated by a sharp peak in C, whereas in the strongly breathing case of $J_1'/J_1 = 0.4$ [see bluish symbols in Fig. 2(a)], P remains zero, but instead, the total chirality χ^{T} develops. One can see from the spin snapshots shown in the top and bottom panels of Fig. 2(c) that the low-temperature phases for $J_1'/J_1 = 1$ and 0.4 are collinear and noncoplanar states, respectively, and that in the latter, three spins on different sublattices are orthogonal to one another. In the noncoplanar state, the spin correlation develops at the ordering vector of $\mathbf{q} = \mathbf{Q}_1$, $\mathbf{Q}_2$, and $\mathbf{Q}_3$ [see Fig. 2(b)], and the topological number is $|n_{\text{sk}}| = 2$ [see the bottom panel of Fig. 2(a)], evidencing that the noncoplanar state is definitely the topological chiral order with a triple-**Q** SkX structure. Here, $n_{\text{sk}} = -2$ and $+2$ correspond to the SkX and anti-SkX with opposite χ^{T}'s, respectively (see Fig. 3), and the ordered
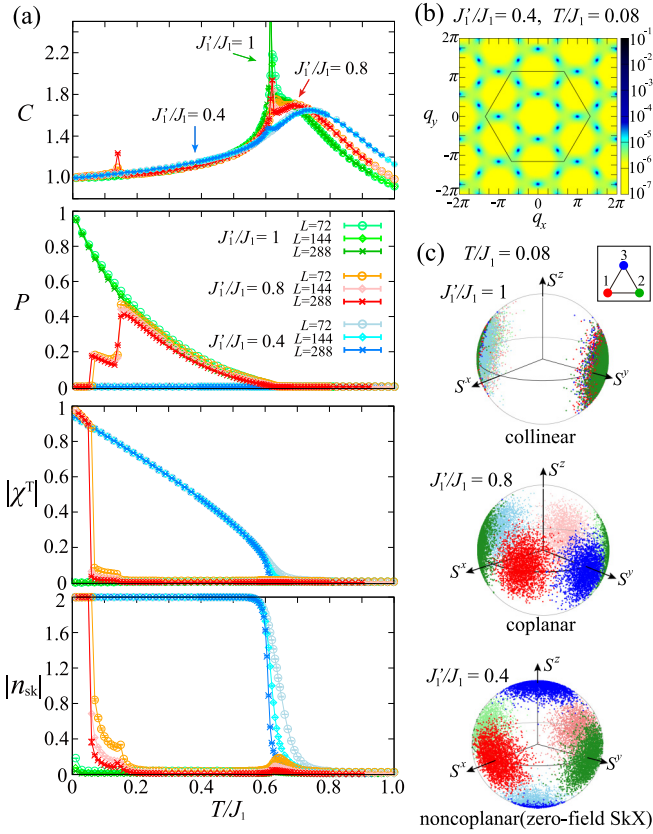
FIG. 2. MC results obtained for $J_3/J_1 = 1.2$ with $J_1 > 0$. (a) Temperature dependence of the specific heat C, the spin collinearity P, the total scalar chirality $|\chi^{\rm T}|$, and the skyrmion number per magnetic unit cell $|n_{\rm sk}|$ (from top to bottom, respectively), where greenish, reddish, and bluish colored symbols correspond to $J_1'/J_1 = 1$, 0.8, and 0.4, respectively. (b) The spin structure factor $\langle|\frac{1}{N}\sum_i \mathbf{S}_i\, e^{i\mathbf{q}\cdot\mathbf{r}_i}|^2\rangle$ obtained in the noncoplanar state at $T/J_1 = 0.08$ for $J_1'/J_1 = 0.4$ and $L = 72$, where the wave number is measured in units of $1/a$ and a hexagon indicates the border of the Brillouin zone. (c) Spin snapshots mapped onto a unit sphere in the collinear state at $J_1'/J_1 = 1$ (top), the coplanar state at $J_1'/J_1 = 0.8$ (middle), and the noncoplanar SkX state at $J_1'/J_1 = 0.4$ (bottom) all of which are obtained at $T/J_1 = 0.08$. Red, green, and blue dots represent spins on sublattices 1, 2, and 3 shown in the inset.

state is the alternative of the two, similarly to other DM-free systems [25].

In the weakly breathing case of $J_1'/J_1 = 0.8$ [see the reddish symbols in Fig. 2(a)], P exhibits two-step sudden drops, suggestive of successive first-order transitions. The higher-temperature and lower-temperature phases correspond to the collinear and noncoplanar states, respectively, and as one can see from the middle panel of Fig. 2(c), the intermediate phase is a coplanar state which turns out to be the one introduced in Fig. 1(b) (for details, see Supplemental Material [54]).

Here, we address the nature of the phase transition. For the noncoplanar state, the chiral symmetry associated with the sign of $\chi^{\rm T}$ is broken. In this chiral phase at $T \neq 0$, spins are not long-ranged ordered and the chirality distribution is uniform (see Supplemental Material [54]), so that the translational symmetry of the underlying lattice is not broken. In this sense, strictly speaking, the "crystal" of SkX is well-
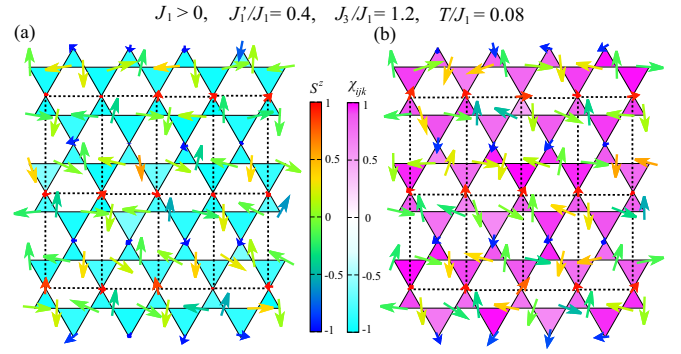

FIG. 3. MC snapshots of the noncoplanar chiral states taken at $T/J_1 = 0.08$ for $J_1'/J_1 = 0.4$ and $J_3/J_1 = 1.2$ with $J_1 > 0$. (a) SkX structure with negative total chirality $\chi^{\rm T}$ and (b) anti-SkX structure with positive $\chi^{\rm T}$. An arrow and its color represent the $S^x S^y$ and S^z components of a spin, respectively, and the color of a triangle represents the local scalar chirality χ_{ijk} defined on each triangle. A unit cell of the skyrmion is indicated by a dotted rectangle.

defined only at $T = 0$ where spins are long-range ordered. It should also be noted that a $\mathbb{Z}_2$-vortex transition [59–61] may be additionally possible as spins are noncollinear in the low-temperature phase. In the transitions into the collinear and coplanar states, a local magnetization $\mathbf{m}_{\rm loc}$ and a local vector chirality $\boldsymbol{\kappa}_{\rm loc}$ defined on each triangle play important roles, respectively, where the manners of their spatial distributions, especially their quadratic correlations between the neighboring triangles, break the lattice translational symmetry (for details, see Supplemental Material [54]).

Now that the emergence of the chiral order having the zero-field SkX structure is confirmed, we will next discuss its mechanism based on the mean-field approximation [62]. We first introduce the Fourier transform $\mathbf{S}_i = \sum_{\mathbf{q}} \mathbf{S}_{\mathbf{q}}^\alpha \exp(i\mathbf{q}\cdot\mathbf{r}_i)$ with the site index $i = (\alpha, \mathbf{r}_i)$ and sublattice indices $\alpha = 1$, 2, and 3 [see the inset of Fig. 1(a)], and pick up the ordering vectors of our interest $\mathbf{Q}_1$, $\mathbf{Q}_2$, and $\mathbf{Q}_3$. Then, the mean field $\langle \mathbf{S}_{\mathbf{q}}^\alpha \rangle$ can be expressed as

$$\langle \mathbf{S}_{\mathbf{q}}^\alpha \rangle = \sum_{\mu=1}^{3} \left(\left[U_{\mathbf{Q}_\mu}^\alpha \right]^* \boldsymbol{\Phi}_{\mathbf{Q}_\mu} \delta_{\mathbf{q},\mathbf{Q}_\mu} + U_{\mathbf{Q}_\mu}^\alpha \boldsymbol{\Phi}_{\mathbf{Q}_\mu}^* \delta_{\mathbf{q},-\mathbf{Q}_\mu} \right), \quad (2)$$

where $U_{\mathbf{Q}_\mu}^\alpha$ represents the αth component of $\mathbf{U}_{\mathbf{Q}_\mu}$ which are given by

$$\mathbf{U}_{\mathbf{Q}_1} = (1, i\varepsilon, i\varepsilon)/\sqrt{1 + 2\varepsilon^2},$$
$$\mathbf{U}_{\mathbf{Q}_2} = (i\varepsilon, 1, i\varepsilon)/\sqrt{1 + 2\varepsilon^2},$$
$$\mathbf{U}_{\mathbf{Q}_3} = (i\varepsilon, i\varepsilon, 1)/\sqrt{1 + 2\varepsilon^2}, \quad (3)$$

with dimensionless coefficient

$$\varepsilon = \frac{J_1 - J_1'}{-\lambda_{\mathbf{Q}_\mu} + J_1 + J_1'},$$
$$\lambda_{\mathbf{Q}_\mu} = \frac{J_1 + J_1' - 4J_3 - \sqrt{(J_1 + J_1' + 4J_3)^2 + 8(J_1 - J_1')^2}}{2}. \quad (4)$$

Note that ε is zero only for $J_1'/J_1 = 1$, and gradually increases with decreasing J_1'/J_1.

In the uniform case of $J_1'/J_1 = 1$ and thereby $\varepsilon = 0$, all the $\mathbf{U}_{\mathbf{Q}_\mu}$'s are orthogonal to one another, so that $\mathbf{\Phi}_{\mathbf{Q}_1}$, $\mathbf{\Phi}_{\mathbf{Q}_2}$, and $\mathbf{\Phi}_{\mathbf{Q}_3}$ correspond to the polarization vectors $\hat{P}_1$, $\hat{P}_2$, and $\hat{P}_3$, respectively. In other words, to make spins exist at each sublattice, the ordered state should be a triple-$\mathbf{Q}$ state involving all the $\mathbf{\Phi}_{\mathbf{Q}_\mu}$'s, and thus, single-$\mathbf{Q}$ and double-$\mathbf{Q}$ states are not realized in the present system. Then, the Ginzburg-Landau (GL) free energy $\mathcal{F}_{\mathrm{GL}}$ is given by $\mathcal{F}_{\mathrm{GL}}/(N/3) = f_2 + f_4 + \delta f_4$ with

$$f_2 = \left[3T + \lambda_{\mathbf{Q}_\mu}\right] \sum_{\mu=1}^{3} \left|\mathbf{\Phi}_{\mathbf{Q}_\mu}\right|^2,$$

$$f_4 = \frac{9T}{20} A_1 \sum_{\mu=1}^{3} \left(\left|\mathbf{\Phi}_{\mathbf{Q}_\mu} \cdot \mathbf{\Phi}_{\mathbf{Q}_\mu}\right|^2 + 2\left[\mathbf{\Phi}_{\mathbf{Q}_\mu} \cdot \mathbf{\Phi}_{\mathbf{Q}_\mu}^*\right]^2\right),$$

$$\delta f_4 = \frac{9T}{20} A_2 \sum_{\mu < \nu} \left(\left|\mathbf{\Phi}_{\mathbf{Q}_\mu}\right|^2 \left|\mathbf{\Phi}_{\mathbf{Q}_\nu}\right|^2 + \sum_{\varepsilon_s = \pm 1} \left|\mathbf{\Phi}_{\mathbf{Q}_\mu} \cdot \mathbf{\Phi}_{\varepsilon_s \mathbf{Q}_\nu}\right|^2\right),$$
(5)

and the coefficients $A_1 = \frac{2(1+2\varepsilon^4)}{(1+2\varepsilon^2)^2}$ and $A_2 = \frac{8\varepsilon^2(2+\varepsilon^2)}{(1+2\varepsilon^2)^2}$. Note that δf_4 is active only in the breathing case of $J_1'/J_1 \neq 1$, i.e., $\varepsilon \neq 0$.

The most stable spin configuration is obtained by minimizing $\mathcal{F}_{\mathrm{GL}}$ under the constraint $\overline{S}^2 = 2 \sum_{\mu=1}^{3} |\mathbf{\Phi}_{\mathbf{Q}_\mu}|^2$. Noting that in the uniform case, $\mathbf{\Phi}_{\mathbf{Q}_\mu}$ corresponds to the polarization vector $\hat{P}_\mu$, we assume $\mathbf{\Phi}_{\mathbf{Q}_\mu} = \frac{\overline{S}}{\sqrt{6}} e^{i\theta_\mu} \hat{P}_\mu$ also in the breathing case. Then, one notices that the relative angles among $\hat{P}_1$, $\hat{P}_2$, and $\hat{P}_3$ are determined only by the δf_4 term which is calculated as

$$\delta f_4 = \frac{T\overline{S}^4}{40} A_2 \left[\frac{3}{2} + (\hat{P}_1 \cdot \hat{P}_2)^2 + (\hat{P}_1 \cdot \hat{P}_3)^2 + (\hat{P}_2 \cdot \hat{P}_3)^2\right].$$
(6)

It is clear from Eq. (6) that in the breathing case of $\varepsilon \neq 0$ and thereby $A_2 > 0$, $\hat{P}_1$, $\hat{P}_2$, and $\hat{P}_3$ become orthogonal to one another to lower the free energy δf_4, resulting in a noncoplanar SkX state. In the uniform case of $\varepsilon = 0$ where the relative angles cannot be fixed because $\delta f_4 = 0$, thermal fluctuations favor the collinear state [57]. Also, the coplanar state is not stabilized at the level of the present GL expansion, so that higher-order terms or thermal fluctuations may be relevant to its stability.

Since the above mean-field result is valid irrespective of the signs of J_1 and J_1', the noncoplanar state should appear even in ferromagnetic J_1 and/or J_1' as long as $J_1 \neq J_1'$ and thereby $\varepsilon \neq 0$. As shown in Fig. 4, this is actually the case: At the lowest temperature of our MC simulations, the noncoplanar SkX state is stable in a wide range of the parameter space except $J_1'/J_1 = 1$ at which the collinear state is realized. We have also checked that this chiral order is relatively robust against a magnetic field and a single-ion anisotropy as well as additional further NN interactions.

For the present zero-field SkX, the sublattice degrees of freedom are fundamentally important because they make it possible to superpose three collinear chains, i.e., sinusoidal modulations, orthogonally, which is in contrast to the con-
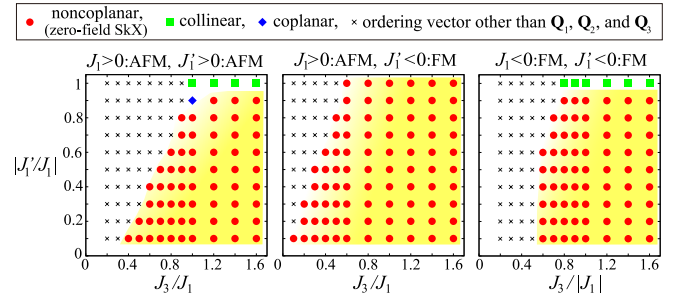

FIG. 4. Parameter dependence of the low-temperature spin structure at $T/|J_1| = 0.01$. For large J_3, the chiral order with the noncoplanar SkX structure is realized irrespective of the sign of J_1 and J_1'.

ventional in-field SkX where three helical modulations are superposed. Although in this work the breathing bond alternation is introduced to select the noncoplanar configuration from numerous energetically degenerate superposition patterns, it might be substituted, on the uniform kagome lattice, by other driving forces such as a positive biquadratic spin interaction [6,30,31].

It is also useful to compare the present two-dimensional breathing kagome system to the associated three-dimensional breathing pyrochlore system. Although in both cases the breathing bond alternation commonly yields noncoplanar topological spin textures, there is a significant difference in the properties of the ordered states. In the breathing pyrochlore system, the hedgehog lattice, an alternating array of magnetic monopoles and antimonopoles of opposite topological charges, can be realized, but the total chirality summed over the whole system is completely canceled out at zero field [50]. In contrast, in the present breathing kagome system, the miniature discrete skyrmions of the same topological charges are condensed, and as a result, the total chirality is nonzero even at zero field, which suggests an interesting aspect of this two-dimensional magnet that in a metallic system, the Hall effect of chirality origin, the so-called topological Hall effect, may be observed even in the absence of an applied magnetic field.

Finally, we will address experimental implications of our results. Although several breathing kagome magnets including $Gd_3Ru_4Al_{12}$ [40] which hosts the in-field SkX have been reported so far [63–70], a magnetic order with commensurate $\mathbf{Q}_1$, $\mathbf{Q}_2$, and $\mathbf{Q}_3$ has not been observed. Nevertheless, in a metallic system, when the ordering vector is governed by the Ruderman-Kittel-Kasuya-Yosida interaction, one may have a chance to realize the commensurate order by tuning the Fermi level or the conduction electron density. If such a candidate material can be synthesized, the topological Hall effect may be observed at zero field as a distinctive signature of the zero-field chiral order with the triple-$\mathbf{Q}$ miniature SkX structure.

On the uniform kagome lattice, the 12-sublattice coplanar state shown in Fig. 1(b) has been reported in the magnetic insulator $BaCu_3V_2O_8(OD)_2$ [71] whose system parameters are consistent with our theory except the breathing lattice structure. If nominal lattice distortions, which might exist in this compound, yield nonequivalent J_1 and J_1', the mechanism presented here could be applied to this class of magnets,

pointing to the possibility of the chiral order in its family compounds.

To conclude, we have theoretically demonstrated that the zero-field chiral order emerges in the form of commensurate triple-$\mathbf{Q}$ SkX in breathing kagome antiferromagnets, where the third NN antiferromagnetic interaction along the bond direction J_3 and the breathing bond alternation are essential. We believe that our study will promote the exploration of different classes of magnetic materials hosting topological spin textures.

[1] N. Nagaosa and Y. Tokura, Nat. Nanotechnol. **8**, 899 (2013).

[2] I. Martin and C. D. Batista, Phys. Rev. Lett. **101**, 156402 (2008).

[3] Y. Akagi and Y. Motome, J. Phys. Soc. Jpn. **79**, 083711 (2010).

[4] K. Barros, J. W. F. Venderbos, G.-W. Chern, and C. D. Batista, Phys. Rev. B **90**, 245119 (2014).

[5] T. Momoi, K. Kubo, and K. Niki, Phys. Rev. Lett. **79**, 2081 (1997).

[6] Y. Akagi, M. Udagawa, and Y. Motome, Phys. Rev. Lett. **108**, 096401 (2012).

[7] A. van Oosterom and J. Strackee, IEEE Trans. Biomed. Eng. **BME-30**, 125 (1983).

[8] A. N. Bogdanov and D. A. Yablonskii, Sov. Phys. - JETP **68**, 101 (1989).

[9] S. D. Yi, S. Onoda, N. Nagaosa, and J. H. Han, Phys. Rev. B **80**, 054416 (2009).

[10] S. Buhrandt and L. Fritz, Phys. Rev. B **88**, 195137 (2013).

[11] S. Muhlbauer, B. Binz, F. Jonietz, C. Pfleiderer, A. Rosch, A. Neubauer, R. Georgii, and P. Boni, Science **323**, 915 (2009).

[12] A. Neubauer, C. Pfleiderer, B. Binz, A. Rosch, R. Ritz, P. G. Niklowitz, and P. Boni, Phys. Rev. Lett. **102**, 186602 (2009).

[13] X. Z. Yu, Y. Onose, N. Kanazawa, J. H. Park, J. H. Han, Y. Matsui, N. Nagaosa, and Y. Tokura, Nature (London) **465**, 901 (2010).

[14] X. Z. Yu, N. Kanazawa, Y. Onose, K. Kimoto, W. Z. Zhang, S. Ishiwata, Y. Matsui, and Y. Tokura, Nat. Mater. **10**, 106 (2011).

[15] S. Heinze, K. von Bergmann, M. Menzel, J. Brede, A. Kubetzka, R. Wiesendanger, G. Bihlmayer, and S. Blugel, Nat. Phys. **7**, 713 (2011).

[16] S. Seki, X. Z. Yu, S. Ishiwata, and Y. Tokura, Science **336**, 198 (2012).

[17] Y. Tokunaga, X. Z. Yu, J. S. White, H. M. Ronnow, D. Morikawa, Y. Taguchi, and Y. Tokura, Nat. Commun. **6**, 7638 (2015).

[18] I. Kezsmarki, S. Bordacs, P. Milde, E. Neuber, L. M. Eng, J. S. White, H. M. Ronnow, C. D. Dewhurst, M. Mochizuki, K. Yanai, H. Nakamura, D. Ehlers, V. Tsurkan, and A. Loidl, Nat. Mater. **14**, 1116 (2015).

[19] Y. Fujima, N. Abe, Y. Tokunaga, and T. Arima, Phys. Rev. B **95**, 180410(R) (2017).

[20] S. Bordacs, A. Butykai, B. G. Szigeti, J. S. White, R. Cubitt, A. O. Leonov, S. Widmann, D. Ehlers, H.-A. Krug von Nidda, V. Tsurkan, A. Loidl, and I. Kezsmarki, Sci. Rep. **7**, 7584 (2017).

[21] T. Kurumaji, T. Nakajima, V. Ukleev, A. Feoktystov, T. H. Arima, K. Kakurai, and Y. Tokura, Phys. Rev. Lett. **119**, 237201 (2017).

[22] A. K. Nayak, V. Kumar, T. Ma, P. Werner, E. Pippel, R. Sahoo, F. Damay, U. K. Robler, C. Felser, and S. S. P. Parkin, Nature (London) **548**, 561 (2017).

[23] M. Kakihana, D. Aoki, A. Nakamura, F. Honda, M. Nakashima, Y. Amako, S. Nakamura, T. Sakakibara, M. Hedo, T. Nakama, and Y. Onuki, J. Phys. Soc. Jpn. **87**, 023701 (2018).

[24] K. Kaneko, M. D. Frontzek, M. Matsuda, A. Nakao, K. Munakata, T. Ohhara, M. Kakihana, Y. Haga, M. Hedo, T. Nakama, and Y. Onuki, J. Phys. Soc. Jpn. **88**, 013702 (2019).

[25] T. Okubo, S. Chung, and H. Kawamura, Phys. Rev. Lett. **108**, 017206 (2012).

[26] A. O. Leonov and M. Mostovoy, Nat. Commun. **6**, 8275 (2015).

[27] S. Z. Lin and S. Hayami, Phys. Rev. B **93**, 064430 (2016).

[28] S. Hayami, S. Z. Lin, and C. D. Batista, Phys. Rev. B **93**, 184413 (2016).

[29] S. Hayami, S. Z. Lin, Y. Kamiya, and C. D. Batista, Phys. Rev. B **94**, 174420 (2016).

[30] R. Ozawa, S. Hayami, and Y. Motome, Phys. Rev. Lett. **118**, 147205 (2017).

[31] S. Hayami, R. Ozawa, and Y. Motome, Phys. Rev. B **95**, 224424 (2017).

[32] S. Z. Lin and C. D. Batista, Phys. Rev. Lett. **120**, 077202 (2018).

[33] S. Hayami and Y. Motome, Phys. Rev. B **99**, 094420 (2019).

[34] Z. Wang, Y. Su, S. Z. Lin, and C. D. Batista, Phys. Rev. Lett. **124**, 207201 (2020).

[35] S. Hayami and Y. Motome, Phys. Rev. B **103**, 024439 (2021).

[36] Z. Wang, Y. Su, S. Z. Lin, and C. D. Batista, Phys. Rev. B **103**, 104408 (2021).

[37] K. Mitsumoto and H. Kawamura, Phys. Rev. B **104**, 184432 (2021).

[38] S. Hayami, T. Okubo, and Y. Motome, Nat. Commun. **12**, 6927 (2021).

[39] T. Kurumaji, T. Nakajima, M. Hirschberger, A. Kikkawa, Y. Yamasaki, H. Sagayama, H. Nakao, Y. Taguchi, T. Arima, and Y. Tokura, Science **365**, 914 (2019).

[40] M. Hirschberger, T. Nakajima, S. Gao, L. Peng, A. Kikkawa, T. Kurumaji, M. Kriener, Y. Yamasaki, H. Sagayama, H. Nakao, K. Ohishi, K. Kakurai, Y. Taguchi, X. Yu, T. Arima, and Y. Tokura, Nat. Commun. **10**, 5831 (2019).

[41] N. D. Khanh, T. Nakajima, X. Z. Yu, S. Gao, K. Shibata, M. Hirschberger, Y. Yamasaki, H. Sagayama, H. Nakao, L. C. Peng, K. Nakajima, R. Takagi, T. Arima, Y. Tokura, and S. Seki, Nat. Nanotechnol. **15**, 444 (2020).

[42] B. Binz and A. Vishwanath, Phys. Rev. B **74**, 214408 (2006).

[43] J. H. Park and J. H. Han, Phys. Rev. B **83**, 184406 (2011).

[44] S-G. Yang, Y-H. Liu, and J. H. Han, Phys. Rev. B **94**, 054420 (2016).

[45] X.-X. Zhang, A. S. Mishchenko, G. De Filippis, and N. Nagaosa, Phys. Rev. B **94**, 174428 (2016).

[46] S. Okumura, S. Hayami, Y. Kato, and Y. Motome, Phys. Rev. B **101**, 144416 (2020).

[47] N. Kanazawa, Y. Nii, X.-X. Zhang, A. S. Mishchenko, G. De Filippis, F. Kagawa, Y. Iwasa, N. Nagaosa, and Y. Tokura, Nat. Commun. **7**, 11622 (2016).

[48] Y. Fujishiro, N. Kanazawa, T. Nakajima, X. Z. Yu, K. Ohishi, Y. Kawamura, K. Kakurai, T. Arima, H. Mitamura, A. Miyake, K. Akiba, M. Tokunaga, A. Matsuo, K. Kindo, T. Koretsune, R. Arita, and Y. Tokura, Nat. Commun. **10**, 1059 (2019).

[49] S. Ishiwata, T. Nakajima, J.-H. Kim, D. S. Inosov, N. Kanazawa, J. S. White, J. L. Gavilano, R. Georgii, K. M. Seemann, G. Brandl, P. Manuel, D. D. Khalyavin, S. Seki, Y. Tokunaga, M. Kinoshita, Y. W. Long, Y. Kaneko, Y. Taguchi, T. Arima, B. Keimer, and Y. Tokura, Phys. Rev. B **101**, 134406 (2020).

[50] K. Aoyama and H. Kawamura, Phys. Rev. B **103**, 014406 (2021).

[51] J.-C. Domenge, P. Sindzingre, C. Lhuillier, and L. Pierre, Phys. Rev. B **72**, 024433 (2005).

[52] J.-C. Domenge, C. Lhuillier, L. Messio, L. Pierre, and P. Viot, Phys. Rev. B **77**, 172413 (2008).

[53] O. Janson, J. Richter, and H. Rosner, Phys. Rev. Lett. **101**, 106403 (2008).

[54] See Supplemental Material at http://link.aps.org/supplemental/10.1103/PhysRevB.105.L100407 for MC results on the spin structures of the triple-**Q** collinear and coplanar states, their order parameters, and notes on the spin configurations of the triple-**Q** coplanar and noncoplanar states, which includes Refs. [55,56].

[55] N. Shannon, K. Penc, and Y. Motome, Phys. Rev. B **81**, 184409 (2010).

[56] H. Kawamura, J. Phys. Soc. Jpn. **79**, 011007 (2010).

[57] V. Grison, P. Viot, B. Bernu, and L. Messio, Phys. Rev. B **102**, 214424 (2020).

[58] L. Messio, C. Lhuillier, and G. Misguich, Phys. Rev. B **83**, 184401 (2011).

[59] H. Kawamura and S. Miyashita, J. Phys. Soc. Jpn. **53**, 4138 (1984).

[60] T. Okubo and H. Kawamura, J. Soc. Phys. Jpn. **79**, 084706 (2010).

[61] K. Aoyama and H. Kawamura, Phys. Rev. Lett. **124**, 047202 (2020).

[62] J. N. Reimers, A. J. Berlinsky, and A. C. Shi, Phys. Rev. B **43**, 865 (1991).

[63] J.-C. Orain, B. Bernu, P. Mendels, L. Clark, F. H. Aidoudi, P. Lightfoot, R. E. Morris, and F. Bert, Phys. Rev. Lett. **118**, 237203 (2017).

[64] L. Clark, J. C. Orain, F. Bert, M. A. De Vries, F. H. Aidoudi, R. E. Morris, P. Lightfoot, J. S. Lord, M. T. F. Telling, P. Bonville, J. P. Attfield, P. Mendels, and A. Harrison, Phys. Rev. Lett. **110**, 207208 (2013).

[65] Y. Haraguchi, C. Michioka, M. Imai, H. Ueda, and K. Yoshimura, Phys. Rev. B **92**, 014409 (2015).

[66] A. Akbari-Sharbaf, R. Sinclair, A. Verrier, D. Ziat, H. D. Zhou, X. F. Sun, and J. A. Quilliam, Phys. Rev. Lett. **120**, 227201 (2018).

[67] M. Zhang, Z. Zhao, W. Zhang, J. Li, X. Huang, and Z. He, Chem. Commun. **56**, 11965 (2020).

[68] M. Takahashi, K. Nawa, D. Okuyama, H. Nojiri, M. D. Frontzek, M. Avdeev, M. Yoshida, D. Ueta, H. Yoshizawa, and T. J. Sato, J. Phys. Soc. Jpn. **89**, 094704 (2020).

[69] H. Tanaka, Y. Fujisawa, K. Kuroda, R. Noguchi, S. Sakuragi, C. Bareille, B. Smith, C. Cacho, S. W. Jung, T. Muro, Y. Okada, and T. Kondo, Phys. Rev. B **101**, 161114(R) (2020).

[70] C. Balz, B. Lake, J. Reuther, H. Luetkens, R. Schöunemann, T. Herrmannsdoürfer, Y. Singh, A. T. M. Nazmul Islam, E. M. Wheeler, J. A. Rodriguez-Rivera, T. Guidi, G. G. Simeoni, C. Baines, and H. Ryll, Nat. Phys. **12**, 942 (2016).

[71] D. Boldrin, B. Fak, E. Canévet, J. Ollivier, H. C. Walker, P. Manuel, D. D. Khalyavin, and A. S. Wills, Phys. Rev. Lett. **121**, 107203 (2018).